Original Article

Vitamin D deficiency inhibits microRNA-196b-5p which regulates ovarian granulosa cell hormone synthesis, proliferation, and apoptosis by targeting *RDX* and *LRRC17*

Ting Wan[1], Huiting Sun[2], Zhilei Mao[1], Lina Zhang[1], Xia Chen[2], Yichao Shi[2], Yuwei Shang[2]

[1]Department of Scientific Research and Education, Changzhou Maternity and Child Health Care Hospital Affiliated to Nanjing Medical University, Changzhou, China; [2]Department of Reproductive Center, The Affiliated Changzhou No. 2 People's Hospital of Nanjing Medical University, Changzhou, China

Contributions: (I) Conception and design: T Wan, H Sun, Y Shi; (II) Administrative support: T Wan, Y Shi, Y Shang; (III) Provision of study materials or patients: T Wan, H Sun; (IV) Collection and assembly of data: T Wan, Y Shang; (V) Data analysis and interpretation: T Wan, Z Mao, L Zhang, X Chen, Y Shi, Y Shang; (VI) Manuscript writing: All authors; (VII) Final approval of manuscript: All authors.

Correspondence to: Yuwei Shang. Department of Reproductive Center, The Affiliated Changzhou No. 2 People's Hospital of Nanjing Medical University, Changzhou 213000, China. Email: shangyuwei_2007@163.com.

Background: In polycystic ovary syndrome (PCOS), ovarian physiology is tightly linked to the metabolic disturbances observed in this disease. Vitamin D (VD) plays an important role in the regulation of ovulatory dysfunction and can influence genes involved in steroidogenesis in granulosa cells (GCs). However, its role in the proliferation and apoptosis of ovarian GCs is unclear. The present study aimed to investigate the role of microRNA-196-5p (miR-196b-5p) in the hormone synthesis, proliferation, and apoptosis of ovarian GCs.

Methods: The abnormal expression of miRNAs in ovarian tissues of VD-deficient mice was analyzed using transcriptome sequencing. The direct target of miR-196b-5p was predict and confirmed by bioinformatics analysis and the dual-luciferase reporter assay. Reverse transcription-quantitative PCR (RT-qPCR) was used to detect the levels of miR-196b-5p, cell proliferation was detected via the CCK8 assay, and cell apoptosis and reactive oxygen species (ROS) were measured via flow cytometry. The levels of radixin (*RDX*), leucine rich repeat containing 17 (*LRRC17*), aromatase (*CYP19A1*), and glucose transporter 4 (*GLUT4*) were detected by performing RT-qPCR or western blot.

Results: We found that miR-196b-5p was significantly downregulated among the 672 miRNAs that were differentially expressed (DE) in VD-deficient mice. In addition, the results demonstrated that downregulated expression of miR-196b-5p significantly increased the level of *RDX* and *LRRC17*, and reduced expression of miR-196b-5p significantly promoted ovarian GC apoptosis and inhibited cell proliferation. Downregulated expression of miR-196b-5p promoted cellular ROS production and inhibited sex hormone production and glucose uptake. Transfection with miR-196b-5p mimics significantly increased the expression of *CYP19A1* and *GLUT4* and decreased the *RDX* and *LRRC17* levels in ovarian GCs.

Conclusions: This study shows that miR-196b-5p can regulate the oxidative stress (OS), glucose uptake, and steroid production pathway of GCs, thus promoting follicular development and maturation. This is a step towards a feasible treatment for PCOS.

Keywords: MicroRNA-196-5p (miR-196b-5p); vitamin D (VD); radixin and leucine rich repeat containing 17 (*RDX* and *LRRC17*); ovarian granulosa cells (ovarian GCs)

Submitted Oct 26, 2021. Accepted for publication Dec 06, 2021.
doi: 10.21037/atm-21-6081
View this article at: https://dx.doi.org/10.21037/atm-21-6081

Introduction

Polycystic ovary syndrome (PCOS) is the most common endocrine disease in premenopausal women, with a prevalence rate of about 6–7%. PCOS is characterized by clinical or biochemical hyperandrogenemia, polycystic ovary morphology, chronic anovulation, or less menstruation (1,2). PCOS is considered hereditary and is caused by a variety of factors, such as increased luteinizing hormone (LH), lack of androgen balance, inflammation, insulin resistance (IR), and oxidative stress (OS) (3). Vitamin D deficiency (VDD) is common in women with PCOS. It is estimated that serum 25-hydroxyvitamin D [25(OH)D] is less than 20 ng/mL in 65–85% of patients with PCOS (4). Notably, VDD may aggravate the symptoms of PCOS because lower concentrations of 25(OH)D are associated with irregular ovulation and menstruation, hyperandrogenemia, IR, hirsutism, low success rate of pregnancy, obesity, and increased risk factors for cardiovascular disease (5,6). There are several methods for the fertility treatment of patients with PCOS. Assisted reproductive technology (ART) is the most commonly used method. In this method, the ovaries are stimulated by exogenous gonadotropin to produce multiple follicles. A large amount of evidence suggests that vitamin D (VD) may have beneficial effects on metabolic/hormonal parameters in PCOS and endometriosis, and seems to be related to the results of in vitro fertilization (IVF) (7-9). In PCOS, ovarian physiology is tightly linked to the metabolic disturbances observed in this disorder. Thus, the beneficial effects of VD on metabolic alterations may translate into better and healthier ovarian physiology.

Radixin (RDX) is a member of the Ezrin-Radixin-moesin (ERM) protein family. It plays the role of membrane cytoskeleton crosslinker in actin rich cell surface structures. Therefore, it is considered to be essential for the organization, cell movement, adhesion, and proliferation of the cortical cytoskeleton. They are also involved in regulating the transporter function of various organs. For example, *RDX* knockout mice showed binding hyperbilirubinemia and liver damage caused by loss of the bilirubin-secreting transporter multidrug resistance-associated protein 2 (MRP2) in the bile duct membrane (10). leucine rich repeat containing 17 (*LRRC17*) is a secretory protein containing 5 leucine-rich repeat domains. It was first characterized in bone metabolism as an inhibitor of receptor activator of nuclear factor-κB ligand (RANKL)-induced osteoclast differentiation. Besides bone metabolism, Malcuit *et al.* found that *LRRC17* was particularly high expressed in oocytes and granulosa cells (GCs) (11). Although human protein maps showed that *LRRC17* is highly expressed in female tissues, but its role in GCs remains unclear.

MicroRNAs (miRNAs) are a class of small non-coding RNAs. It is estimated that they regulate the mRNA translation of more than 70% of protein-coding genes and are widely involved in normal and disease states (12). In addition, miRNAs are involved in the regulation of GCs proliferation, apoptosis, and steroid production, and their imbalance may play an important role in the pathogenesis of PCOS (13,14). Some studies have determined that VD_3 affects the expression of genes involved in steroid production in normal ovarian GCs (15-17). However, there are no studies showing the effects of miRNAs on GC proliferation, apoptosis, OS, glucose uptake, or the steroid production pathway under VDD conditions. In this study, for the first time, we analyzed the transcriptome of the ovaries in a VDD mouse model and evaluated the effect of miR-196b-5p on the hormone synthesis, proliferation, and apoptosis of GCs by targeting *RDX* and *LRRC17*. We present the following article in accordance with the ARRIVE reporting checklist (available at https://dx.doi.org/10.21037/atm-21-6081).

Methods

Animal procedure

Female C57BL/6J mice (age, 3 weeks; weight, 12–18 g) were obtained from Carvens, Inc. (Changzhou, China) [animal certificate No. SCXK(SU)2016-0010]. Mice were housed in a specific pathogen-free environment under standard housing conditions with controlled temperature (22±1 ℃) and humidity (52%±5%). The mice were exposed to a 12 h light/dark cycle and were able to access a specified amount of food and water at will. All animal experiments in this study were carried out in strict accordance with the Regulations for the Administration of Affairs Concerning Experimental Animals approved by the State Council of the People's Republic of China (11-14-1988). The animal experimental design and protocols were approved by the Institutional Animal Care and Use Committee (IACUC) of Nanjing Medical University (approval number: 2020-62).

The experimental group and procedures of mice were described previously (18). In the present study, a total of 30 mice were used, of which 5 were the control group and 5 were VD deficient group, and repeat for 3 times independently to eliminate the difference between experiments at different batches. Briefly, after feeding for 8 weeks with a VD-deficient (25 IU VD_3/kg; cat. no.

D119289, Dyets) or control diet (5,000 IU VD_3/kg; cat. no. D119290, Dyets), mice were sacrificed by cervical dislocation. Before analysis, the serum samples were centrifuged at 6,000 rpm for 5 minutes and stored at –20 ℃. Serum 25(OH)D_3 levels were measured using an enzyme-linked immunosorbent assay (ELISA) kit (cat. no. AC-57SF1; Immunodiagnostic Systems, Ltd.). Determination of serum levels of follicle stimulating hormone (FSH), LH, estradiol, and testosterone was performed using commercial ELISA kits (Tongwei Bio, Shanghai, China). Ovarian tissues were collected in 4% formalin for hematoxylin and eosin (H&E) staining or RNAlater (Invitrogen, USA) for RNA sequencing by Genewiz, Inc. (Suzhou, China), as described previously (19).

Cell culture

KNG cells were obtained from Nanjing Medical University and cultured in Dulbecco's Modified Eagle's Medium/ F12 (DMEM/F12; Gibco, USA) supplemented with 10% fetal bovine serum (FBS; Gibco, USA) in an incubator with 5% CO_2 at 37 ℃. At the time of passage, the cells were first digested with 0.25% trypsin (containing EDTA). Subsequently, the cell suspension was evenly distributed into a cell culture flask, with the whole medium supplemented to 6 mL per flask. Cell culture was then continued for subsequent experiments.

Cell counting kit-8 (CCK-8) assay

KGN cells were cultured at a density of 0.3-1×10^5 cells/well in 24-well culture plates and transfected with 50 nM miR-196b-5p mimics/ mimics control and miR-196b-5p inhibitor/ inhibitor control using Lipofectamine 2000 (Invitrogen, Carlsbad, CA, USA) according to instruction of the manufacturer. After transfection, cells in log phase were trypsinized and resuspended in complete medium, and 100 μL of cell suspension was added to the culture plate at a density of 5×10^3 cells/per well. After culture for 0, 24, 48, and 72 h, 100 μL of DMEM solution containing 10% CCK-8 reagent (Solarbio, Beijing, China) was added to each well, followed by incubation in an incubator for 2 h in the dark. Lastly, absorbance at 450 nm was detected using a preheated microplate reader.

Flow cytometry

Cells were first cultured in 0.5% Roswell Park Memorial Institute-1640 (RPMI-1640) medium (HyClone, South Logan, UT, USA) for 48 h. Then, the medium was replaced with 10% RPMI-1640 medium for another 48 h. Subsequently, the cells were collected in 3 mL tubes with approximately 2×10^6 cells per tube. After washing twice with phosphate-buffered saline (PBS) solution, the cells were fixed with 70% alcohol and placed in a refrigerator at –20 ℃ for 24–48 h. After routine PI staining, DNA content was measured by AttuneNxT flow cytometry (Thermo, USA). Finally, the percentage of each stage of the cell cycle was analyzed by CytExpert software.

Reverse transcription-quantitative PCR (RT-qPCR)

Total RNA was extracted from KGN cells by Trizol reagent (Invitrogen, Carlsbad, CA, USA). Using 100 ng of total RNA as a template, cDNA was obtained through the TaqMan microRNA reverse transcription kit (Applied Biosystems, Carlsbad, CA, USA). According to the manufacturer's instructions, the qPCR reaction was performed using the ABI7900 real-time PCR system (ABI, Carlsbad, CA, USA). PCR primers (*Table 1*) were designed and synthetized by Sangon Biotech (Shanghai, China). Actin served as the internal reference (U6 served as the internal reference for endonuclear RNA and miR-196b-5p). The threshold was selected at the lowest point of each logarithmic magnification curve to obtain the threshold cycle (Ct) value of each reaction tube, and the data were analyzed by the $2^{-\Delta\Delta Ct}$ method.

Western blot assay

First, 200 μL protein lysate (including 2 μL protease inhibitor and 2 μL phosphatase inhibitor) was added to each well. The mixture was stirred well on ice until the cells were completely lysed. A 5× loading buffer containing β-mercaptoethanol was added and mixed, the mixture was boiled for 15 minutes, then stored at –20 ℃ for use. The extracted protein samples were separated by 10% polyacrylamide gel and transferred to a polyvinylidene fluoride (PVDF) membrane (Millipore, Billerica, MA, USA). After blocking with 5% bovine serum albumin (BSA) for 2 h, the membrane was incubated with a primary antibody overnight. Antibodies for *LRRC17*, *RDX*, glucose transporter 4 (*GLUT4*), aromatase (*CYP19A*), and *GAPDH* were obtained from Abmart Inc. (Shanghai, China). The next day, the membranes were incubated with the corresponding secondary antibody for 1 h. Finally,

Table 1 Primers used for real-time PCR analysis

Gene	Sequences (5'-3')
U6 R	GTCGTATCCAGTGCAGGGTCCGAGGTATTCGCACTGGATACGACAAAATA
U6 F	AGAGAAGATTAGCATGGCCCCTG
MiR-196b-5p R	CTCAACTGGTGTCGTGGAGTCGGCAATTCAGTTGAGCCCAACAA
MiR-196b-5p F	ACACTCCAGCTGGGTAGGTAGTTTCCTGTT
Actin F	TGGACTTCGAGCAAGAGATG
Actin R	GAAGGAAGGCTGGAAGAGTG
RDX F	CACCTCCACCACCACCAGTC
RDX R	TTCAGCATTATTCTCATCGTGTTCATC
LRRC17 F	TAAACAAACTCACCACCCTCTTACTG
LRRC17 R	TGGACTTTCACACTTGGCGTAG
CYP19A1 F	GACACCTCTAACACGCTCTTCTTG
CYP19A1 R	AGTCCATACATTCTTCCAGTTTCTCTTC
GLUT4 F	GTATCATCTCTCAGTGGCTTGGAAG
GLUT4 R	TAGGAGGCAGCAGCGTTGG

R, reverse; F, forward; miR, microRNA; *RDX*, radixin; *LRRC17*, leucine rich repeat containing 17; *CYP19A1*, aromatase; *GLUT4*, glucose transporter 4.

immunoreactive bands were visualized by the enhanced chemiluminescence (ECL) method.

Luciferase reporter assay

The binding sites of miR-196b-5p were predicted by a bioinformatics website (http://www.targetscan.org). The 293T cells were cultured at a density of $(0.3–1)\times10^5$ cells/well in 24-well culture plates and transfected with 2 μg of dual-luciferase reporter construct pmirGLO-*LRRC17/RDX*-wt/mut, and co-transfected with 50 nM miR-196b-5p mimics/mimics control using Lipofectamine 2000 (Invitrogen, Carlsbad, CA, USA) according to the manufacturer's instructions. At 4 h post-transfection, the transfection medium was removed and replenished with medium containing 10% FBS (Gibco, Rockville, MD, USA). At 48 h post-transfection, luciferase activity was measured using the Dual-Luciferase Reporter Gene Assay Kit (Beyotime, Shanghai, China).

Statistical analysis

All experiments were repeated at least 3 times. The data were expressed as mean ± standard deviation (SD) and analyzed by GraphPad Prism software using the *t*-test or one-way analysis of variance (ANOVA). $P<0.05$ was considered to be statistically significant.

Results

Clinical parameters, endocrine parameters, and transcriptome sequencing analysis of VD-deficient mice

To illustrate the effect of VDD, mouse serum 1,25-$(OH)_2D_3$ levels were measured by the ELISA method and mouse ovaries were sectioned and stained with H&E. The ovarian sections of the control group showed that the peripheral cortex had a large number of follicles at different developmental stages. The structure of the ovarian medulla was normal (*Figure 1A*). In contrast, the ovaries obtained from VD-deficient mice showed a distorted shape (*Figure 1B*). VD-deficient mice (n=5) had 1,25-$(OH)_2D_3$ levels of 19.56±1.51 ng/mL compared with control mice (n=5) that had 1,25-$(OH)_2D_3$ levels of 62.34±2.70 ng/mL ($P<0.01$; *Figure 1C*). For the measurement of ovarian function in the pathology of cyst formation, the levels of serum estradiol, progesterone, and testosterone were evaluated by ELISA. The results showed that the testosterone level of VD-

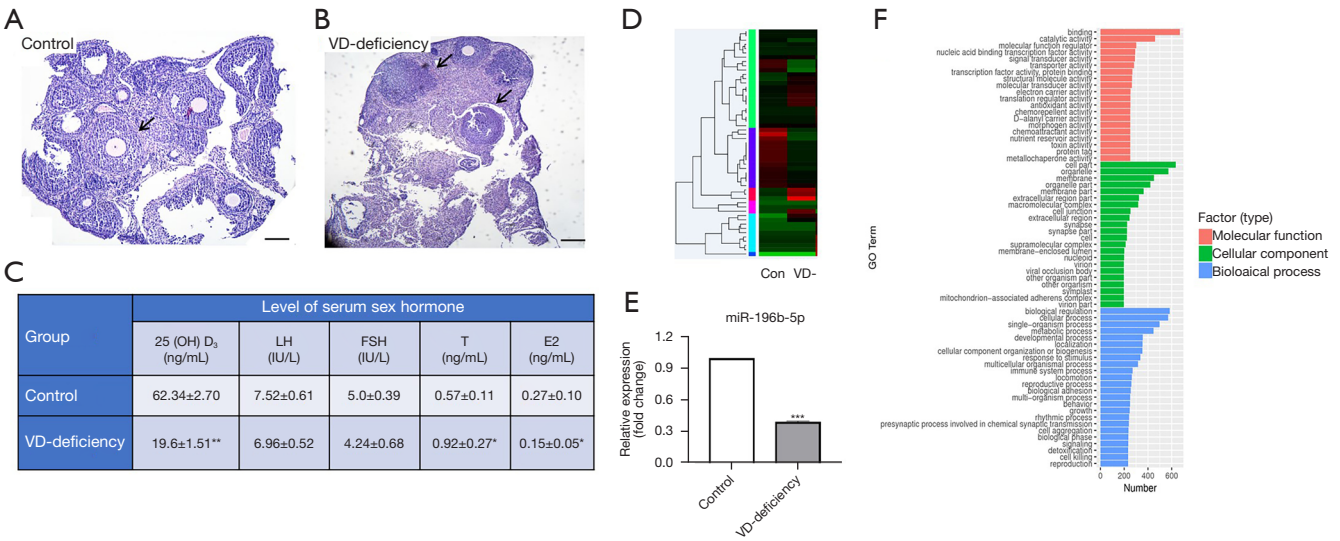

Group	Level of serum sex hormone				
	25 (OH) D_3 (ng/mL)	LH (IU/L)	FSH (IU/L)	T (ng/mL)	E2 (ng/mL)
Control	62.34±2.70	7.52±0.61	5.0±0.39	0.57±0.11	0.27±0.10
VD-deficiency	19.6±1.51**	6.96±0.52	4.24±0.68	0.92±0.27*	0.15±0.05*

Figure 1 Morphological appearance, endocrine parameters, and transcriptome sequencing analysis of control and of VD-deficient mouse ovaries. (A) Control ovaries revealed several follicles (arrow) in various developmental stages stained with H&E. (B) VD-deficient mouse ovaries showed atretic folli and follicular cysts (arrows) on the ovary surface stained with H&E. Scale bar: 50 μm. (C) The serum 25(OH)D_3 and hormone levels in control and VD-deficient mice (*P<0.05, **P<0.01). (D) MiRNA clustering analysis of VD-deficient mice using a heat map to show the significantly downregulated genes. (E) MiR-196b-5p expression levels were significantly upregulated in the VD-deficient group compared with the control group (***P<0.001). (F) GO functional enrichment analysis. VD, vitamin D; H&E, hematoxylin and eosin; 25(OH)D_3, 25-hydroxyvitamin D3; miRNA, microRNA; miR, microRNA; GO, Gene Ontology; LH, luteinizing hormone; FSH, follicle stimulating hormone; T, testosterone; E2, estradiol.

deficient mice was significantly higher than that of the control group, while the estradiol level was significantly lower than that of the control group (P<0.05). However, there was no significant difference in terms of LH and FSH levels between the two groups (P>0.05; *Figure 1C*).

In order to explore the mechanism of 1,25-$(OH)_2D_3$ in improving ovarian function, RNA was extracted from the ovaries and sequenced, and the gene expression levels of the VD-deficient group and control group were analyzed. RNA-seq showed that the expression of 6,543 genes changed in VD-deficient ovaries. A total of 672 differentially expressed (DE) miRNAs were identified, while transcripts per million (TPM) values of >4 in both libraries were retained for further analysis (*Figure 1D*, available online: https://cdn.amegroups.cn/static/public/atm-21-6081-01.xlsx). Among them, 33 miRNAs were reported to have log2-fold change and false discovery rate ≤0.05 in upregulation or downregulation, regardless of miRNA abundance. Furthermore, 17 miRNAs were significantly upregulated while 16 miRNAs were downregulated in the ovarian tissue of VD-mice compared with controls (*Table 2*, available online: https://cdn.amegroups.cn/static/public/atm-21-6081-02.xlsx). RNA-seq demonstrated that miR-196b-5p was significantly downregulated in the ovaries of VD-deficient mouse models. MiR-196b-5p expression in VD-deficient mouse ovarian tissue was verified via qPCR, which showed significantly lower expression compared with the control group (P<0.001; *Figure 1E*). These data showed that the transcriptional spectrum changed significantly in the absence of 1,25-$(OH)_2D_3$ to change ovarian function.

In order to explore the effects of 1,25-$(OH)_2D_3$ on the intracellular functions and signaling pathways of ovarian cells, we used Gene Ontology (GO) and Kyoto Encyclopedia of Genes and Genomes (KEGG) pathway analysis to determine the biological functions and signal pathways of DE mRNAs enrichment. DE mRNAs were significantly enriched in biological processes (BPs), including various developmental processes, migration processes, and small molecular catabolism processes (*Figure 1F*). Among the top 20 items of significant enrichment, 11 items belonged to the BP category [the first 10 items were biological regulation, cellular process, single cell BP, metabolic process, localization, development process, cellular component

Table 2 Top 10 miRNAs and their target genes with significant differences in the ovaries of VD-deficient and control mice

MiRNA	Target genes
Downregulation	Upregulation
Novel miRNA-84	*Arfgef1, Adgrb3, Khdrbsz, Aff3, Ankrd44, Vwc2l, Fn1, Tns1, Wdfy1, Dock10*
Novel miRNA-7	*Slc13a3, Rbak, Ascc1, Timeless, Inpp46*
mmu-miR-200c-5p	*Nxph1, Cox10, Ifrd1*
mmu-miR-196b-5p	*Nsmf, Ctdc1, Katna1, Map3k5, Plazg6, Rpgr*
Novel miRNA-142	*Zc3hc1, Trip4, Arhgap12*
Upregulation	Downregulation
mmu-miR-378d	*Sntg1, Sgk3, Ppp1r42, Cspp1, A830018L16Rik, Slco5a1, Ncoa2, Eya1, Terf1, Stua2*
mmu-miR-669o-5p	*Sntg1, Sgk3, Adgr63, Fam168b, Ankrd44, Dpp10, Nckap5, Tem163, Zranb3, Brinp3*
Novel miRNA-118	*Cspp1, Adgrb3, Slc39a10, Abi2, Vwc2l, Smarcal1, Pid1, Nckap5, Nav1, Colgalt2*
Novel miRNA-54	*Ntm, Afhgap42*
mmu-miR-466i-5p	*Arhgef4, Cdk15, Zfp142, Clgt1a9, Lrrfip1, Clasp1, Nckap5, Zranb3, Kgl1, Astn1*

MiRNA, microRNA; VD, vitamin D.

Table 3 Top 10 KEGG metabolic pathways of miRNA target genes

Pathway ID	Pathway	DEGs with pathway annotation (n=9,509), n (%)	All genes with pathway annotation (n=17,443), n (%)	P value
ko04912	GnRH signaling pathway	192 (2.02)	269 (1.54)	3.85E-09
ko04020	Calcium signaling pathway	349 (3.67)	497 (2.85)	1.33E-13
ko04014	Ras signaling pathway	462 (4.86)	689 (3.95)	3.22E-12
ko04310	Wnt signaling pathway	258 (2.71)	400 (2.29)	1.70E-05
ko04910	Insulin signaling pathway	288 (3.03)	448 (2.57)	8.81E-06
ko04010	MAPK signaling pathway	563 (5.92)	785 (4.50)	1.67E-24
ko04911	Insulin secretion	207 (2.18)	285 (1.63)	7.88E-11
ko04114	Oocyte meiosis	221 (2.32)	306 (1.75)	4.74E-11
ko04210	Apoptosis	156 (1.64)	254 (1.46)	1.07E-02
ko04151	PI3K-Akt signaling pathway	610 (6.41)	960 (5.50)	2.36E-09

KEGG, Kyoto Encyclopedia of Genes and Genomes; DEGs, differentially expressed genes.

(CC) tissue or biogenesis, stimulus response, multicellular BP, immune system process], 7 items belonged to the CC category (cell part, organelle, membrane part, membrane part, extracellular region part, macromolecular complex), while two items belonged to the molecular function (MF) category (binding, catalytic activity). Thus, most of the differentially expressed genes (DEGs) were related to cell metabolism and development in BPs.

DE mRNAs also exhibited significant involvement in various pathways, primarily including the PI3K-Akt signal pathway, MAPK signal pathway, HTLV-I infection, RAS signal pathway, endocytosis, proteoglycan in cancer, regulation of actin cytoskeleton, insulin signal pathway, tight junction, and GnRH signal pathway (*Table 3*, available online: https://cdn.amegroups.cn/static/public/atm-21-6081-03.xlsx).

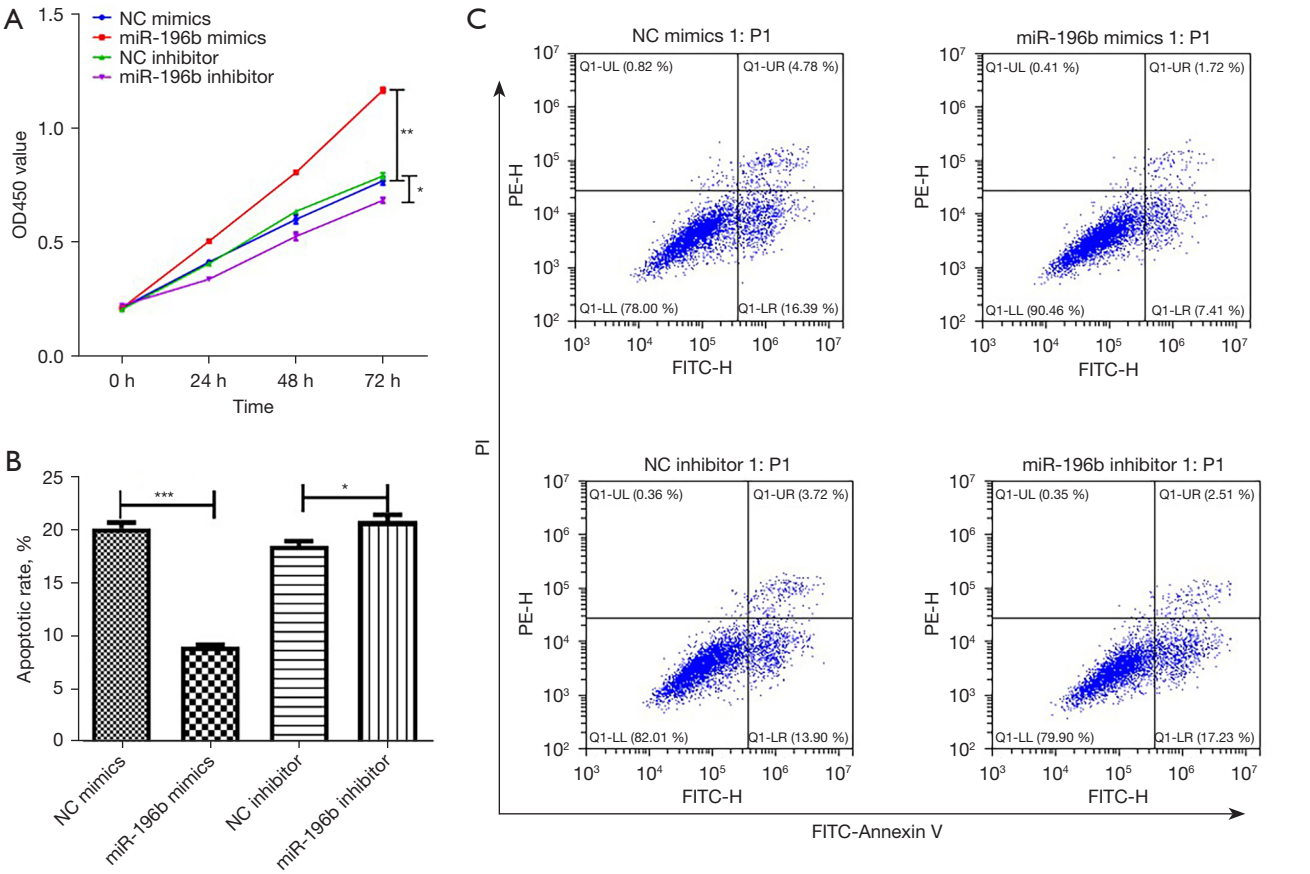

Figure 2 Overexpression of miR-196b-5p promoted KGN cell proliferation and inhibited KGN cell apoptosis. (A) The proliferation ability of KGN cells transfected with miR-196b mimics or miR-196b inhibitor was determined by CCK-8 assays (n=3). (B,C) Flow cytometry was used to determine cell apoptosis, and overexpression of miR-196b-5p could significantly inhibit apoptosis (n=3). The results were representative of 3 independent experiments. Statistical analysis was performed by Student's *t*-test. Data were shown as the mean ± SD. *P<0.05, **P<0.01, ***P<0.001 *vs.* control group. MiR, microRNA; CCK-8, cell counting kit-8; SD, standard deviation; NC, negative control.

MiR-196b-5p promoted cell proliferation and suppressed cell apoptosis

In order to verify the hypothesis that miR-196b-5p may be involved in GC proliferation, KGN cells were transiently transfected with miR-196b-5p mimics, miR-196b-5p inhibitor, or controls. As illustrated in *Figure 2A*, the CCK-8 assays revealed that upregulation of miR-196b-5p resulted in a promotion of KGN cell proliferation. Flow cytometry assays revealed that low expression of miR-196b-5p could significantly inhibit KGN cell apoptosis (*Figure 2B,2C*).

MiR-196b-5p reduced OS and promoted glucose uptake and steroidogenesis

Some studies have shown that apoptosis of various cell types, including GCs, may be related to increased levels of reactive oxygen species (ROS) (20). We determined the effect of miR-196b-5p on the total ROS content. As shown in *Figure 3A,3B*, miR-196b-5p mimics significantly decreased the amount of ROS in KGN cells compared to NC mimics (P<0.001). In contrast, miR-196b-5p inhibitor treatment increased the ROS in KGN cells compared to negative control (NC) inhibitor treatment (P<0.05). The energy requirement of normal folliculogenesis mainly depends on GC glucose uptake in the surrounding tissue through the GLUT on the cell membrane and the production of pyruvate and lactic acid through glycolysis as the main energy source. Next, we studied the glucose uptake capacity of miR-196b-5p-overexpressed KGN cells. The glucose content in the supernatants of the cells was

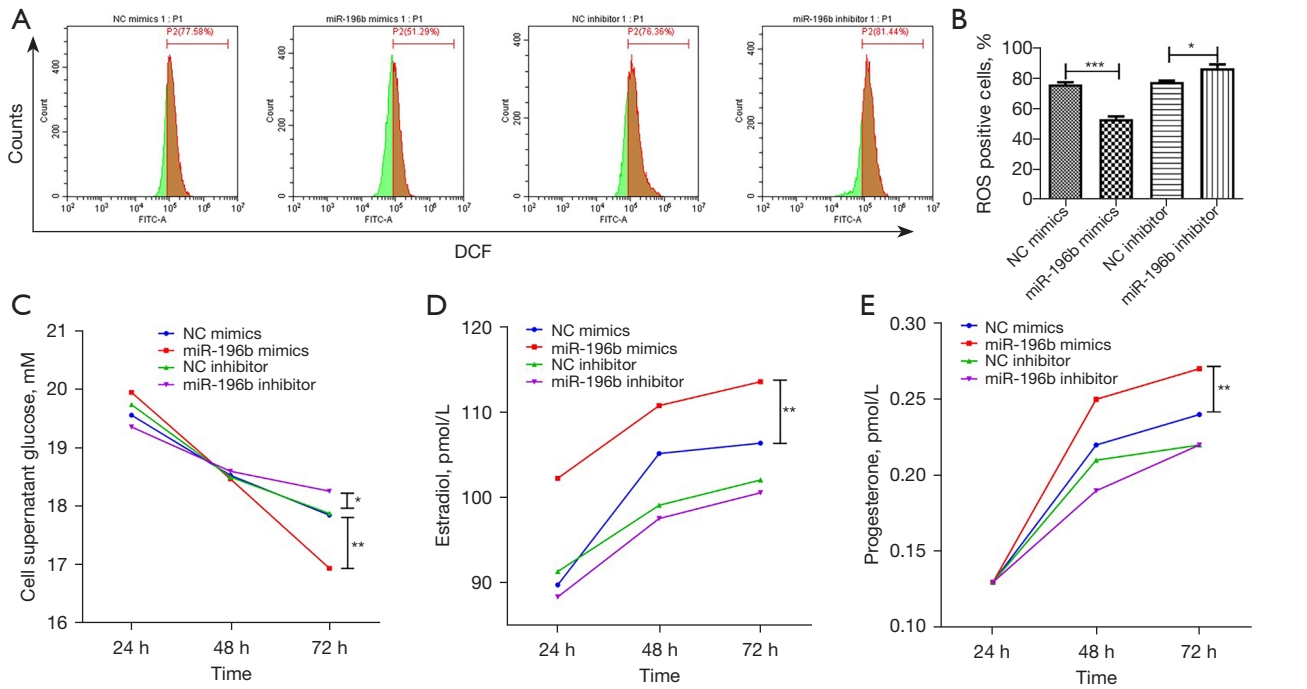

Figure 3 Effect of miR-196b-5p overexpression on ROS production, glucose uptake, and sex steroid production in KGN cells. (A,B) Overexpression of miR-196b-5p inhibits ROS production and interferes with miR-196b-5p to promote ROS production. (C) Overexpression of miR-196b-5p promotes KGN cell glucose uptake. (D,E) Overexpression of miR-196b-5p promotes estradiol and progesterone production. *P<0.05, **P<0.01, ***P<0.001 *vs.* control group. MiR, microRNA; ROS, reactive oxygen species; NC, negative control.

examined after the cells were cultured for 24, 48, and 72 h. There was no significant difference in glucose content among all groups at 24–48 h. At 72 h, glucose uptake became stronger in the miR-196b-5p mimics group (P<0.01) and weaker in the miR-196b-5p inhibitor group (P<0.05; *Figure 3C*).

Next, we investigated the effect of miR-196b-5p overexpression on the production of progesterone and estradiol by KGN cells. Cells were incubated with certain concentrations of miR-196b-5p mimics or inhibitor for 24, 48, and 72 h. Secretions of both estradiol (*Figure 3D*) and progesterone (*Figure 3E*) were increased by miR-196b-5p mimics in KGN cells at 48–72 h (P<0.01). There were no significant differences in estradiol and progesterone among the miR-196b-5p inhibitor and NC inhibitor groups at 24–72 h.

To strengthen these data, we investigated the effect of miR-196b-5p on the mRNA expression of *LRRC17*, *RDX*, *GLUT4* and *CYP19A* gene. RT-PCR results identified that the miR-196b-5p expression levels were significantly upregulated in the miR-196b-5p mimics group compared with the NC group (P<0.01). Moreover, miR-196b-5p expression was significantly downregulated in the miR-196b-5p inhibitor group compared with the inhibitor NC group (P<0.05). These results indicated the successful overexpression or knockdown of miR-196b-5p in KGN cells (*Figure 4A*). As shown in *Figure 4B*,*4C*, we found similar effects of miR-196b-5p mimics on mRNA *LRRC17* and *RDX* expression in KGN cells. *GLUT4* mRNA expression was significantly increased in the miR-196b-5p mimic group and significantly increased in the inhibitor group (*Figure 4D*,*4E*). The results of western blotting are consistent with those of RT-PCR. The expression levels of *LRRC17* and *RDX* were decreased after miR-196b-5p overexpression, while the expression levels of *GLUT4* and *CYP19A* were increased after miR-196b-5p overexpression (*Figure 4F*). These results further verified that miR-196b-5p directly regulated *LRRC17* or *RDX* and promoted glucose uptake and sex steroid production by *GLUT4* and *CYP19A* in KGN cells.

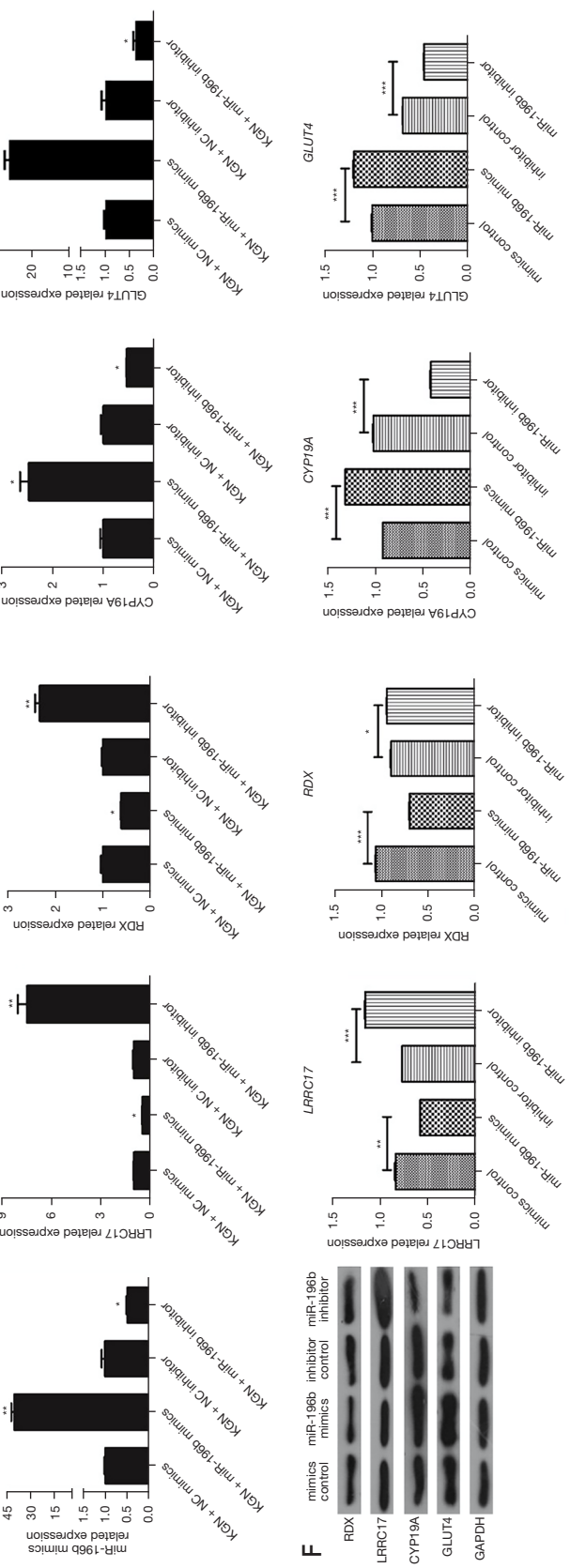

Figure 4 Effect of miR-196b-5p overexpression on *RDX*/*LRRC17* and *GLUT4*/*CYP19A* expression in KGN cells. (A) RT-PCR results showed that miR-196b-5p was significantly upregulated in the mimic group and significantly downregulated in the inhibitor group. (B-E) *LRRC17* and *RDX* mRNA expression levels were decreased significantly in the mimic group and increased significantly in the inhibitor group, while *GLUT4* and *CYP19A* mRNA expression levels increased significantly in the mimic group and decreased significantly in the inhibitor group. (F) Western blot analyses of *LRRC17*, *RDX*, *GLUT4*, and *CYP19A* expression levels in KGN cells transfected with miR-196b-5p mimics or inhibitors. Expression levels of *LRRC17* and *RDX* were decreased after miR-196b-5p overexpression, and the expression levels of *GLUT4* and *CYP19A* were increased after miR-196b-5p overexpression. *P<0.05, **P<0.01, ***P<0.001 *vs.* respective NC. MiR, microRNA; *RDX*, radixin; *LRRC17*, leucine rich repeat containing; *GLUT4*, glucose transporter 4; *CYP19A*, aromatase; NC, negative control.

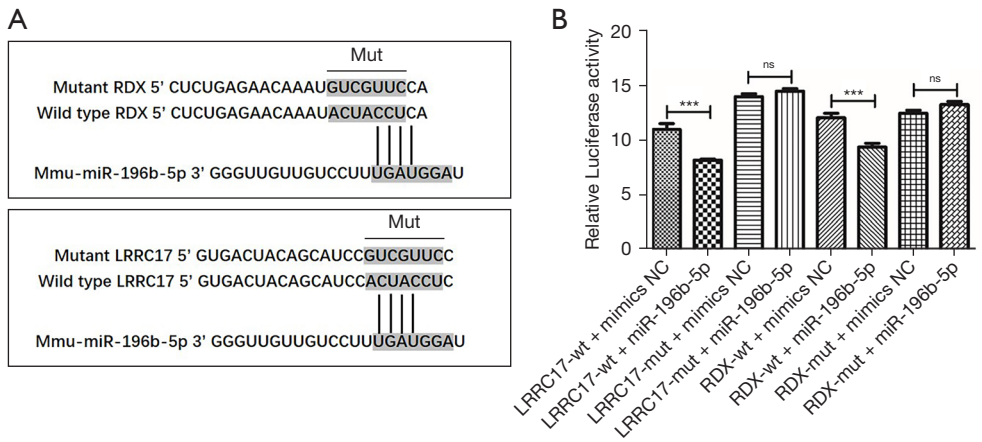

Figure 5 *RDX* and *LRRC17* were target genes of miR-196b-5p. (A) Prediction of binding sites between *RDX/LRRC17* and miR-196b-5p by TargetScan. (B) Dual-luciferase reporter assay results further verified the existence of a targeted relationship between miR-196b-5p and RDX/LRRC17. ***P<0.001 *vs.* NC group. *RDX*, radixin; *LRRC17*, leucine rich repeat containing; miR, microRNA; NC, negative control; ns, non significant.

Prediction of target genes and luciferase reporter assays

In order to study the mechanism of miR-196b-5p in inhibiting the proliferation of GCs, we used TargetScan to find its potential target genes. *RDX* and *LRRC17*, which are closely related to cell proliferation, have sparked our interest. To verify the prediction of TargetScan, we constructed a luciferase reporter vector containing predicted *RDX* and *LRRC17* 3'UTR binding sites (*Figure 5A*). The results showed that overexpression of miR-196b-5p resulted in a significant decrease in luciferase activity after co-transfection with *RDX* or *LRRC17* WT 3'UTR, while there was no change in luciferase activity after co-transfection with *RDX* or *LRRC17* MUT 3'UTR (P<0.001, P>0.05; *Figure 5B*).

Discussion

In this study, a mouse model of VDD was established as previously described (19), and transcriptome sequencing analysis revealed that miR-196b-5p was abnormally downregulated in the ovarian tissues of VD-deficient mice, which was further confirmed using RT-qPCR of the extracted ovarian tissues from the mice. Functional experiments further demonstrated that overexpression of miR-196b-5p mimics facilitated cell proliferation and inhibited apoptosis in KGN cells. It is reported that increasing the level of miR-196b-5p can be achieved by downregulating type I collagen α 1 chain (*COL1A1*), which significantly inhibited proliferation and migration of MDA-MB-231 and MDA-MB-468 cells in breast cancer (21). In addition, miR-196b-5p is associated with some pathological changes, such as lung adenocarcinoma (22), hepatocellular carcinoma (23), keloid (24), and colorectal cancer (25), among others. It is also reported that mouse miR-196b can specifically target the 5' noncoding region of insulin 2 splicing isoforms. The RNA binding protein HUD, which inhibits insulin translation, was replaced by miR-196b, indicating that miR-196b upregulates insulin 2 translation (26). They found that increased miR-196b expression induced by glucose may be another mechanism by which glucose stimulates insulin synthesis. The role of miR-196b in ovarian GCs is worthy of further study.

Our study showed that overexpression of miR-196b-5p resulted in a promotion of KGN cell proliferation and low expression of miR-196b-5p could significantly inhibit KGN cell apoptosis. MiR-196b-5p is a positive factor related to the proliferation of ovarian GCs. In addition, *RDX* and *LRRC17* were direct targets of miR-196b-5p in KGN cells. Overexpression of miR-196b-5p led to significantly decreased luciferase activity by co-transfection with *RDX* or *LRRC17* WT 3'UTR, while there was no change with *RDX* or *LRRC17* MUT 3'UTR. It has been reported that *RDX* is a direct target of miR-196b-5p in human gastric cancer (27). Studies (28) have shown that miR-200b regulates the proliferation and invasion of breast cancer cells by targeting *RAD* expression. The overexpression of miR-200b inhibits the expression of *RAD* and reduces the proliferation and invasion of breast cancer cells. Chen

et al. (29) demonstrated that silencing the expression of *RAD* in pancreatic cancer cells significantly inhibited cell proliferation and tumorigenicity *in vivo*. *RDX* seems to be a positive factor in cell proliferation, but this is not reflected in our experimental results. Decreased *LRRC17* has been shown to be a serum risk marker for osteoporotic fracture in the spines of postmenopausal women (30). Song *et al.* (31) demonstrated that the modulation of the *LRRC17* gene may delay or even restore the balance of osteogenic and adipogenic differentiation in autologous bone marrow mesenchymal stem cells derived from patients with idiopathic necrosis of the femoral head (INFH). There are few reports on the function of *LRRC17* in ovarian GCs, though so far one study has demonstrated that *LRRC17* could be a prognostic gene in ovarian cancer as it regulates cancer cell viability through the p53 pathway (32).

Hyperinsulinemia and IR play a central role in the pathogenesis of PCOS. They can affect the severity of clinical features, though are not associated with the existence of obesity. *GLUT4* is a member of the GLUT family, which is preferentially expressed in muscle and adipose tissue. GLUT4 is responsible for insulin-stimulated glucose uptake, which may lead to IR (33). Our study showed that overexpression of miR-196b-5p can significantly reduce the expression of *GLUT4*, resulting in a decrease in glucose uptake. PCOS is a highly prevalent endocrine-metabolic disorder associated with IR. The decrease of glucose uptake and utilization by skeletal muscle and adipocytes caused by the decrease of *GLUT4* expression or activity is an important molecular basis of IR. A prospective cross-sectional study showed that IR secondary to PCOS insulin-mediated decreased glucose uptake and increased insulin secretion was partly due to decreased *GLUT4* expression in adipocytes without a compensatory increase in *GLUT1* expression (34). The analysis of signaling components of the IRS/PI3K/AKT pathway showed that the expression of *GLUT4* was significantly decreased in PCOS patients and the IR control group (35). Their results point to a new mechanism by which miR-93 regulates insulin-stimulated glucose uptake and demonstrates that the upregulated expression of miR-93 in all women with IR with or without PCOS may be the cause of IR in this syndrome. The *CYP19A* gene responsible for aromatase P450 is located on chromosome 15q21.2 and is necessary for estrogen formation. It is reported that obese and lean women with PCOS have low aromatase activity. Studies have also shown that interruption of the steroid production pathway caused by androgen overdose is a key factor in abnormal follicle formation and dominant follicular selection failure in hyperandrogen-induced PCOS women. The key enzyme for the production of estradiol in the ovaries is *CYP19A1*, which is involved in the transformation of androgen to estradiol in GCs (36). In our study, secretions of both estradiol and progesterone were increased by miR-196b-5p mimics in KGN cells, as well as the expression of *CYP19A*. In addition, our study showed miR-196b-5p mimics significantly decreased the amount of ROS in KGN cells. OS is an important inducer of ovarian senescence, which leads to the decline of the reproductive ability of humans and different animals. We showed that miR-196b-5p reduced the ROS content. Unfortunately, we did not detect the expression of ROS-related proteins and the PI3K-Akt signaling pathway associated with IR. In fact, obesity or IR may increase the OS of these cells. It will be interesting to determine whether miR-196b-5p is an effective antioxidant molecule. Recent reports have identified a close interaction between VDD and OS in exacerbating the pathophysiology of PCOS (37,38).

In conclusion, we found that miR-196b-5p was significantly downregulated in the ovaries of VDD mice. In KGN cells, after inhibiting the expression of miR-196b-5p, cell proliferation decreased and apoptosis increased. At the same time, it was found that the decreased expression of *CYP19A* and *GLUT4* led to a decrease in glucose uptake and the secretion of estrogen and progesterone. After inhibiting the expression of miR-196b-5p, the increase of intracellular ROS content indicated the increase of OS. It has been proven that *RDX* and *LRRC17* are the target genes miR-196b-5p (*Figure 6*). This is a preliminary but pioneering study to elucidate the functions of miR-196b-5p, *RDX*, and *LRRC17* in KGN cells and their relationships. In the meantime, there are some limitations in our study. First, we performed *in vitro* experiments in KGN cell lines, so we were unable to predict the *in vivo* effect of miR-196b-5p on ovarian function. Second, a large number of PCOS patients are needed to further verify the expression of miR-196b-5p, *RDX*, and *LRRC17*. Therefore, we plan to continue this experiment in our subsequent work.

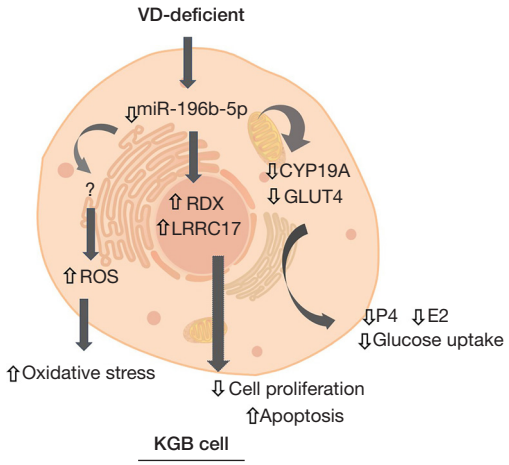

Figure 6 Representative schema of the effects of miR-195b-5p on VDD. MiR, microRNA; VDD, vitamin D deficiency; VD, vitamin D; ROS, reactive oxygen species; RDX, radixin; LRRC17, leucine rich repeat containing; *GLUT4*, glucose transporter 4; *CYP19A*, aromatase; E2, estradiol.

Acknowledgments

Funding: This study was funded by the Youth Program of Changzhou Health Commission (QN201942), the Young Scientists Foundation of Changzhou No. 2 People's Hospital (2019K009) and Project of Youth Scientists of Changzhou Health Commission (CZQM2020100).

Footnote

Reporting Checklist: The authors have completed the ARRIVE reporting checklist. Available at https://dx.doi.org/10.21037/atm-21-6081

Data Sharing Statement: Available at https://dx.doi.org/10.21037/atm-21-6081

Conflicts of Interest: All authors have completed the ICMJE uniform disclosure form (available at https://dx.doi.org/10.21037/atm-21-6081). The authors have no conflicts of interest to declare.

Ethical Statement: The authors are accountable for all aspects of the work in ensuring that questions related to the accuracy or integrity of any part of the work are appropriately investigated and resolved. All animal experiments in this study were carried out in strict accordance with the Regulations for the Administration of Affairs Concerning Experimental Animals approved by the State Council of the People's Republic of China (11-14-1988). The animal experimental design and protocols were approved by the Institutional Animal Care and Use Committee (IACUC) of Nanjing Medical University (approval number: 2020-62).

References

1. Escobar-Morreale HF. Polycystic ovary syndrome: definition, aetiology, diagnosis and treatment. Nat Rev Endocrinol 2018;14:270-84.
2. Ajmal N, Khan SZ, Shaikh R. Polycystic ovary syndrome (PCOS) and genetic predisposition: a review article. Eur J Obstet Gynecol Reprod Biol X 2019;3:100060.
3. Khan MJ, Ullah A, Basit S. Genetic basis of polycystic ovary syndrome (PCOS): current perspectives. Appl Clin Genet 2019;12:249-60.
4. Lerchbaum E, Rabe T. Vitamin D and female fertility. Curr Opin Obstet Gynecol 2014;26:145-50.
5. Lerchbaum E, Obermayer-Pietsch B. Vitamin D and fertility: a systematic review. Eur J Endocrinol 2012;166:765-78.
6. Faghfoori Z, Fazelian S, Shadnoush M, et al. Nutritional management in women with polycystic ovary syndrome: a review study. Diabetes Metab Syndr 2017;11 Suppl 1:S429-32.
7. Fung JL, Hartman TJ, Schleicher RL, et al. Association of vitamin D intake and serum levels with fertility: results from the Lifestyle and Fertility Study. Fertil Steril 2017;108:302-11.
8. Rudick B, Ingles S, Chung K, et al. Characterizing the influence of vitamin D levels on IVF outcomes. Hum Reprod 2012;27:3321-7.
9. Rudick BJ, Ingles SA, Chung K, et al. Influence of vitamin D levels on in vitro fertilization outcomes in donor-recipient cycles. Fertil Steril 2014;101:447-52.
10. Kikuchi S, Hata M, Fukumoto K, et al. Radixin

deficiency causes conjugated hyperbilirubinemia with loss of Mrp2 from bile canalicular membranes. Nat Genet 2002;31:320-5.
11. Malcuit C, Trask MC, Santiago L, et al. Identification of novel oocyte and granulosa cell markers. Gene Expr Patterns 2009;9:404-10.
12. Paul P, Chakraborty A, Sarkar D, et al. Interplay between miRNAs and human diseases. J Cell Physiol 2018;233:2007-18.
13. Sirotkin AV, Lauková M, Ovcharenko D, et al. Identification of microRNAs controlling human ovarian cell proliferation and apoptosis. J Cell Physiol 2010;223:49-56.
14. Tu J, Cheung AH, Chan CL, et al. The role of microRNAs in ovarian granulosa cells in health and disease. Front Endocrinol (Lausanne) 2019;10:174.
15. Lee CT, Wang JY, Chou KY, et al. 1,25-dihydroxyvitamin D3 increases testosterone-induced 17beta-estradiol secretion and reverses testosterone-reduced connexin 43 in rat granulosa cells. Reprod Biol Endocrinol 2014;12:90.
16. Merhi Z, Doswell A, Krebs K, et al. Vitamin D alters genes involved in follicular development and steroidogenesis in human cumulus granulosa cells. J Clin Endocrinol Metab 2014;99:E1137-45.
17. Bakhshalizadeh S, Amidi F, Alleyassin A, et al. Modulation of steroidogenesis by vitamin D3 in granulosa cells of the mouse model of polycystic ovarian syndrome. Syst Biol Reprod Med 2017;63:150-61.
18. Li P, Xu X, Cao E, et al. Vitamin D deficiency causes defective resistance to Aspergillus fumigatus in mice via aggravated and sustained inflammation. PLoS One 2014;9:e99805.
19. Sun H, Shi Y, Shang Y, et al. MicroRNA 378d inhibits Glut4 by targeting Rsbn1 in vitamin D deficient ovarian granulosa cells. Mol Med Rep 2021;23:369.
20. Yang H, Xie Y, Yang D, et al. Oxidative stress-induced apoptosis in granulosa cells involves JNK, p53 and Puma. Oncotarget 2017;8:25310-22.
21. Zhu X, Rao X, Yao W, et al. Downregulation of MiR-196b-5p impedes cell proliferation and metastasis in breast cancer through regulating COL1A1. Am J Transl Res 2018;10:3122-32.
22. Xu Q, Xu Z. miR-196b-5p promotes proliferation, migration and invasion of lung adenocarcinoma cells via targeting RSPO2. Cancer Manag Res 2020;12:13393-402.
23. Zhai H, Zhang X, Chen S, et al. RP5-1120P11.3 promotes hepatocellular carcinoma development via the miR-196b-5p-WIPF2 axis. Biochem Cell Biol 2020;98:238-48.
24. Yang J, Deng P, Qi Y, et al. NEAT1 knockdown inhibits keloid fibroblast progression by miR-196b-5p/FGF2 axis. J Surg Res 2021;259:261-70.
25. Xin H, Wang C, Chi Y, et al. MicroRNA-196b-5p promotes malignant progression of colorectal cancer by targeting ING5. Cancer Cell Int 2020;20:119.
26. Panda AC, Sahu I, Kulkarni SD, et al. miR-196b-mediated translation regulation of mouse insulin2 via the 5'UTR. PLoS One 2014;9:e101084.
27. Tsai MM, Wang CS, Tsai CY, et al. MicroRNA-196a/-196b promote cell metastasis via negative regulation of radixin in human gastric cancer. Cancer Lett 2014;351:222-31.
28. Yuan J, Xiao C, Lu H, et al. miR-200b regulates breast cancer cell proliferation and invasion by targeting radixin. Exp Ther Med 2020;19:2741-50.
29. Chen SD, Song MM, Zhong ZQ, et al. Knockdown of radixin by RNA interference suppresses the growth of human pancreatic cancer cells in vitro and in vivo. Asian Pac J Cancer Prev 2012;13:753-9.
30. Hong N, Kim BJ, Kim CH, et al. Low plasma level of leucine-rich repeat-containing 17 (LRRc17) is an independent and additive risk factor for osteoporotic fractures in postmenopausal women. J Bone Miner Res 2016;31:2106-14.
31. Song D, Wu ZS, Xu Q, et al. LRRC17 regulates the bone metabolism of human bone marrow mesenchymal stem cells from patients with idiopathic necrosis of femoral head through Wnt signaling pathways: a preliminary report. Exp Ther Med 2021;22:666.
32. Oh CK, Park JJ, Ha M, et al. LRRC17 is linked to prognosis of ovarian cancer through a p53-dependent anti-apoptotic function. Anticancer Res 2020;40:5601-9.
33. Zhang N, Liu X, Zhuang L, et al. Berberine decreases insulin resistance in a PCOS rats by improving GLUT4: dual regulation of the PI3K/AKT and MAPK pathways. Regul Toxicol Pharmacol 2020;110:104544.
34. Ezeh U, Chen IY, Chen YH, et al. Adipocyte expression of glucose transporter 1 and 4 in PCOS: Relationship to insulin-mediated and non-insulin-mediated whole-body glucose uptake. Clin Endocrinol (Oxf) 2019;90:542-52.
35. Panghiyangani R, Soeharso P, Andrijono, et al. CYP19A1 gene expression in patients with polycystic ovarian syndrome. J Hum Reprod Sci 2020;13:100-3.
36. Chen YH, Heneidi S, Lee JM, et al. miRNA-93 inhibits GLUT4 and is overexpressed in adipose tissue of polycystic ovary syndrome patients and women with insulin resistance. Diabetes 2013;62:2278-86.

37. Kyei G, Sobhani A, Nekonam S, et al. Assessing the effect of MitoQ10 and Vitamin D3 on ovarian oxidative stress, steroidogenesis and histomorphology in DHEA induced PCOS mouse model. Heliyon 2020;6:e04279.
38. Safaei Z, Bakhshalizadeh SH, Nasr Esfahani MH, et al. Effect of vitamin D3 on mitochondrial biogenesis in granulosa cells derived from polycystic ovary syndrome. Int J Fertil Steril 2020;14:143-9.

(English Language Editor: C. Betlzar)

Cite this article as: Wan T, Sun H, Mao Z, Zhang L, Chen X, Shi Y, Shang Y. Vitamin D deficiency inhibits microRNA-196b-5p which regulates ovarian granulosa cell hormone synthesis, proliferation, and apoptosis by targeting RDX and LRRC17. Ann Transl Med 2021;9(24):1775. doi: 10.21037/atm-21-6081

